Published in final edited form as:
Int J Radiat Oncol Biol Phys. 2013 August 1; 86(5): 969–977. doi:10.1016/j.ijrobp.2013.04.028.

Molecular Imaging of the ATM Kinase Activity

Terence M. Williams, M.D., Ph.D.[1,*], **Shyam Nyati, Ph.D.**[2,3], **Brian D. Ross, Ph.D.**[3,4], and **Alnawaz Rehemtulla, Ph.D.**[2,3,4]

[1]The Department of Radiation Oncology, The Ohio State University, Columbus, OH 43235, U.S.A.

[2]The Department of Radiation Oncology, University of Michigan Medical Center, Ann Arbor MI 48109, U.S.A

[3]The Center for Molecular Imaging, University of Michigan Medical Center, Ann Arbor MI 48109, U.S.A

[4]Department of Radiology, University of Michigan Medical Center, Ann Arbor MI 48109, U.S.A

Abstract

Purpose—Ataxia telangiectasia mutated (ATM) is a serine/threonine kinase critical to the cellular DNA-damage response, including from DNA double-strand breaks (DSBs). ATM activation results in the initiation of a complex cascade of events including DNA damage repair, cell cycle checkpoint control, and survival. We sought to create a bioluminescent reporter that dynamically and non-invasively measures ATM kinase activity in living cells and subjects.

Methods and Materials—Using the split luciferase technology we constructed a hybrid cDNA, ATM-reporter (ATMR), coding for a protein that quantitatively reports on changes in ATM kinase activity through changes in bioluminescence.

Results—Treatment of ATMR expressing cells with ATM inhibitors resulted in a dose dependent increase in bioluminescence activity. In contrast, induction of ATM kinase activity upon irradiation resulted in a decrease in reporter activity that correlated with ATM and Chk2 activation by immunoblotting in a time-dependent fashion. Nuclear targeting improved ATMR sensitivity to both ATM inhibitors and radiation, while a mutant ATMR (lacking the target phosphorylation site) displayed a muted response. Treatment with ATM inhibitors and siRNA-targeted knockdown of ATM confirm the specificity of the reporter. Using reporter expressing xenografted tumors demonstrated the ability of ATMR to report in ATM activity in mouse models which correlated in a time-dependent fashion with changes in Chk2 activity.

Conclusions—We describe the development and validation of a novel, specific, non-invasive bioluminescent reporter that enables monitoring of ATM activity in real-time *in vitro* and *in vivo*. Potential applications of this reporter include the identification and development of novel ATM inhibitors or ATM-interacting partners through high-throughput screens, and *in vivo* pharmacokinetic/pharmacodynamic studies of ATM inhibitors in pre-clinical models.

[*]corresponding author: Alnawaz Rehemtulla, PhD, Department of Radiation Oncology, University of Michigan, 109 Zina Pitcher Place, BSRB, A528, Ann Arbor, MI 48109-2200, Phone (734) 764-4209, Fax (734) 763-5447, alnawaz@umich.edu.

Conflict of Interest: None.

Introduction

Cells have evolved remarkable pathways to maintain genomic integrity and have developed responses to DNA damage from a number of different stresses, including UV or ionizing radiation. While it appears that disruption of pathways that survey and repair DNA damage may be an important event in the acquisition of mutations which ultimately lead to carcinogenesis, many cancers still maintain active DNA damage response (DDR) pathways important for cell survival. Numerous tumor types show activation in DDR pathways in the early stages of tumorigenesis, and some tumors demonstrate heightened DNA repair, which can be a common mechanism of therapy resistance [2,3]. Central to activation of this pathway is ATM kinase [9,13], which is efficiently and quickly activated upon exposure to ionizing radiation. Several studies have implied that ATM kinase may be a suitable target for anti-neoplastic therapy [4,13]. When activated by ionizing radiation, ATM phosphorylates a number of downstream effector proteins, including p53, Chk2, Chk1, gamma-H2A.X, NBS1/nibrin, BRCA1 and Rad 17. ATM-mediated activation of Chk2 occurs by phosphorylation at Thr68, resulting in stabilization of p53, activation of BRCA-1 for DNA homologous recombination repair, and degradation/sequestration of CDC25A and CDC25C phosphatases to induce cell cycle arrest [1,11,13]. Although ATM activation leads to cell cycle arrest, ATM levels stay constant during the cell cycle [6].

In an effort to provide novel biological insights into this pathway, we describe the development of an ATM kinase reporter (ATMR), a firefly luciferase-based reporter for real-time, non-invasive, dynamic monitoring of the ATM kinase activity in cells and living subjects. We demonstrate that the ATMR reports the activation and inactivation of ATM kinase activity. Furthermore, we show that the ATMR has improved sensitivity after being targeted to the nucleus, exhibits significant specificity to ATM kinase, and can be utilized to monitor the effects of ATM inhibitors *in vivo*.

Materials and Methods

Construction of the ATM reporter (ATMR)

The bioluminescent Akt reporter (BAR) plasmid backbone [16] was used for the construction of the ATM reporter using forward CTAGAGGAGGAGCTGGAGGGTTAGAGACAGTGTCCACTCAGGAACTCTATTC TATTC; and reverse CCGGGAATAGAATAGAGTTCCTGAGTGGACACTGTCTCTAACCCTCCAGCTC CTCCT primer. The ATMR-NLS construct and ATMR-NLSmut construct were created by site-directed mutagenesis. All the clones were sequence verified.

Generation of stable cell lines

HEK-293 (human embryonic kidney) and D54 (human glioblastoma) cells were maintained in DMEM or RPMI, respectively, (Invitrogen, Grand Island, NY) with 10% etal bovine serum, 1% glutamine, and 0.1% penicillin/streptomycin. To generate stable cell lines, the ATMR-reporter plasmids were transfected into the cells and selected using 200 μg/ml G418 (Invitrogen).

Antibodies, chemicals, and siRNA

Rabbit polyclonal antibodies to ATM, phospho-ATM (Ser1981), phospho-Chk2 (Thr68), phospho-H2A.X (Ser139), and GAPDH were purchased from Cell Signaling Technology (Danvers, MA). A goat anti-luciferase antibody was purchased from Chemicon/Millipore (Billerica, MA) while luciferin was from Biosynth (Itasca, IL). CGK733 and KU-55933 were obtained from EMD Chemicals, USA. ATM siGENOME SMARTpool and control

siRNA were purchased from Dharmacon (Lafayette, CO). For siRNA transfection, cells were plated in 6-well plates and transfection was carried out with Lipofectamine 2000 (Invitrogen), according to the manufacturer's instructions.

Immunoblotting

Cell lysates were prepared in RIPA lysis buffer (1% NP-40, 150mM NaCl, 50mM Tris-HCL pH 7.4, 0.25% Na-deoxycholate, 1 mM EDTA) supplemented with 1x protease inhibitor. Protein concentration was determined with a Dc Protein Assay Kit (BioRad, Hercules, CA). Proteins were resolved by SDS/PAGE and probed with primary antibodies at a dilution of 1:1,000 while GAPDH was used at 1:10,000.

Bioluminescence imaging

Cells stably expressing the reporter were plated at equal density in 12-well clear-bottom plates. Live-cell luminescent imaging was performed on IVIS 200 imaging system (Caliper Life Science, Hopkinton, MA) 5 min after adding D-luciferin (100μg/ml). ROI values were calculated and analyzed using LivingImage 3.0 (Caliper Life Science). Each experiment was done in triplicate and repeated multiple times. Single cell bioluminescent imaging was performed on a Cellgraph bioluminescent imager (ATTO, Asakusa, Japan), after pre-incubation with D-luciferin (200 μg/ml final concentration) for 5 min, followed by a 30 min image acquisition time.

Experimental Radiation

All irradiation was performed at 320 kVp, 10 mA using a Kimtron IC-320 orthovoltage irradiator (Kimtron Medical, CT). For cell experiments, a 20 × 24 cm cone was used at a source-to-surface distance (SSD) of 50cm at a dose rate of approximately 434 cGy/min. For animal irradiation, a 6×8 cm cone was used at an SSD of 40cm, at a dose rate of approximately 138 cGy/min. Mice were anesthetized with isofluorane and placed in cardboard restraints. Flank irradiation was carried out using a custom cut-out lead secondary collimator.

Immunocytochemistry

Cells grown on glass coverslips were fixed with 3.5% paraformaldehyde followed by chilled methanol. Cells were blocked by 1% BSA/1% donkey serum and incubated with 1:50 anti-Luciferase antibody, washed and incubated with Cy3-anti-Goat antibody (Jackson ImmunoResearch, West Grove, PA). Cells were again washed and mounted with SlowFade/Prolong with DAPI (Invitrogen). Images were acquired with a Nikon fluorescence microscope with an excitation wavelength of 533 nm.

Tumor xenograft and in vivo bioluminescence imaging

All animal procedures were approved by the University Committee on Use and Care of Animals (UCUCA). Four to six weeks old athymic CD-1 female mice were obtained from Charles River Laboratories (Wilmington, MA) and acclimatized for at least one week before use. The mice were injected sub-cutaneously with 2×10^6 D54-ATMR cells in each flank. Tumors were allowed to grow to the size of 100–150 mm^3. Mice were injected intraperitoneally with vehicle control (DMSO), CGK-733, KU-55933 (25 mg/kg) or irradiated with 5 Gy to each flank. Bioluminescence was acquired on Xenogen IVIS Spectrum system (Caliper Life Science, Hopkinton, MA) after injecting 400μg/100μl of D-luciferin at baseline (-3h) as well as 1, 4, and 8 hours after drug administration.

Results

Construction of bioluminescent ATM reporter

The ATM kinase reporter (ATMR) was constructed by inserting a 12 amino acid sequence derived from Chk2 in the BAR backbone (Fig. 1a [16]). The Chk2 peptide was flanked by short linker sequences, a phosphopeptide binding domain (FHA2) [5], and N-terminal (N-Luc) and C-terminal (C-Luc) domains of the firefly luciferase [10]. The functional basis of the reporter is demonstrated in Fig. 1B. In the presence of ATM kinase activity, the Chk2 target peptide is phosphorylated, resulting in interaction with the FHA2 domain, producing stearic constraints which inhibit functional reconstitution of the luciferase. In the absence of ATM activity such as inhibitors, siRNA mediated knockdown or phosphatase, the Chk2 consensus sequence is hypophosphorylated, allowing for luciferase enzyme reconstitution and *increased bioluminescent activity*.

ATM reporter responds to ATM inhibition and radiation

In order to test the response of the ATMR, we treated HEK-293 cells expressing ATMR with ATM inhibitors, caffeine and CGK733 [12,14] which resulted in a substantial increase in bioluminescence over vehicle treated cells (Fig. 2A). Treatment of cells for one hour with 3 mM caffeine resulted in a 1.7-fold increase in activity compared to vehicle-treated cells ($p<0.01$). Likewise, treatment of cells with 10 μM, but not with 1 μM of CGK733, resulted in 1.6-fold increase in reporter activity. The IC50 for CGK733 was estimated to be 200nM for ATM in *in-vitro* kinase assay [15].

To evaluate the response of ATMR to radiation, we treated cells with 0.5, 2 and 4 Gy of radiation and acquired bioluminescence activity after 15 and 60 min (Supplemental figure-e1). Since radiation activates ATM, we expected decreased reporter activity. As expected there was a dose dependent decrease in the ATMR activity with increasing radiation (asterisk, $p<0.05$ compared to 0 Gy). For additional assays we selected 2 Gy of ionizing radiation as this is the most clinically relevant dose. As demonstrated in Fig. 2B, 2Gy irradiation resulted in a statistically significant decline in reporter activity within the first 15 minutes ($p<0.05$), maximal between 30 and 60 minutes (~12% decline), before returning to near control levels by 2 hours.

To verify that the reporter functions in an independent cell line, we created a stable line using D54 human glioblastoma cells. Treatment of D54-ATMR cells for one hour with 10 μM of CGK733 resulted in 1.7-fold reporter activity ($p<0.01$, Fig. 2C). These cells exhibited maximal decline in reporter activity by 2 Gy irradiation within 30 minutes, which returned to near baseline by 2 hours (Fig. 2D).

These results were validated by Western blotting in 293-ATMR cells in parallel experiments. Upon irradiation, there was an increase in ATM and Chk2 activation within the first 15 minutes as measured by increased phospho-ATM (Ser1981) and phospho-Chk2 (Thr68), which is maximal between 30 and 60 minutes (Fig. 2E), and decline thereafter.

Improvement of ATMR sensitivity by addition of a nuclear localization sequence

Since ATM functions predominantly as a nuclear kinase, a nuclear-targeted ATMR construct was generated to improve sensitivity. A nuclear localization signal (NLS) [8] was added to the N terminus of the ATMR (Fig 3A; ATMR-NLS). In parallel, a mutant construct (ATMR-NLSmut) was made where ST67/68 sites were mutated to alanine (Fig. 3A bottom). Stable 293-ATMR-NLS and 293-ATMR-NLSmut cells were generated and immunocytochemistry was performed with a luciferase antibody to confirm nuclear enrichment. As shown in Fig. 3B, 293-ATMR cells demonstrate immunofluorescence

predominantly throughout the cytoplasm, with lower expression in the nucleus (top). The addition of the NLS markedly increases reporter targeting to the nucleus, with much lower levels of the reporter construct present in a peri-nuclear fashion in the cytoplasm (Fig. 3B bottom). Cellgraph imaging was used to detect bioluminescent signals at the subcellular level. 293-ATMR cells showed diffuse signal throughout, (Fig. 3C, left) while 293-ATMR-NLS cells demonstrated bioluminescent signal localized to the nucleus (Fig. 3C, right).

In order to evaluate if ATMR-NLS demonstrated improved sensitivity, we treated 293-ATMR, 293-ATMR-NLS, 293-ATMR-NLSmut, and control 293-Luc cells with an ATM inhibitor and acquired luminescence. As shown in Fig. 4A, treatment of 293-ATMR cells with 10 μM of CGK733 resulted in 1.5-fold increase in reporter activity while 293-ATMR-NLS cells demonstrated a 1.9-fold increase in reporter activity over 293-Luc control cells, as well as a statistically significant increase in reporter activity compared to 293-ATMR cells. 293-ATMR-NLSmut cells showed only a 1.3-fold increase in reporter activity over 293-Luc cells. The ATMR-NLS construct was also evaluated in response to ATM activation after ionizing radiation. 293-ATMR-NLS cells unlike 293-ATMR-NLSmut cells, showed more significant changes in bioluminescent activity compared to control cells, correlating with greater reporter sensitivity.

The activity of the ATMR-NLS reporter was also determined using a specific chemical inhibitor of ATM, KU-55933 which has an IC50 of 13nM against ATM in *in-vitro* kinase assay [7]. 293-Luc, 293-ATMR-NLS, and 293-ATMR-NLSmut cells were treated with increasing concentrations of KU-55933 or vehicle (DMSO), and fold bioluminescent reporter activities were normalized to 293-Luc (Fig. 5). There was a dose-dependent increase in reporter activity from 10 to 50 μM in the ATMR-NLS cells that was substantially attenuated in the ATMR-NLSmut cells. Maximal reporter activation was observed at 50 μM KU-55933 (1.8-fold for ATMR-NLS cells, 1.3-fold for ATMR-NLSmut cells).

Finally, targeted knockdown of ATM kinase was also performed using 293-Luc and 293-ATMR-NLS cells were transfected with control or ATM specific siRNA (Fig. 5B, top). Control and ATM siRNA transfected cells were irradiated to stimulate ATM activity. As shown in Fig. 5B (bottom), pre-treatment with ATM siRNA significantly abrogated the response of 293-ATMR-NLS cells to ionizing radiation, with about a 50% decline in reporter response, consistent with Western blot analysis. Taken together, this data provides evidence that the reporter is acting in response to ATM inhibition or activation, in an ATM-specific manner.

In vivo imaging of ATM kinase activity

In order to confirm the functionality of ATM reporter *in vivo*, D54-ATMR tumors were established in nude mice and treated with DMSO (control), CGK733 or KU-55933 (both 25 mg/kg) and monitored bioluminescence over time. We observed significant increases in reporter activation in a time-dependent fashion in response to both KU-55933 and CGK733 treatment (Fig. 6A, 6B). There was an immediate increase in reporter activation 1 hour after injection, which was sustained and maximal at 4 hours. However, KU-55933 was markedly more effective in inducing reporter activation compared to CGK733 given at the same dose and method of administration. With KU-55933 treatment, reporter activation increased 9.0-fold at 1 and 4 hours, before dropping down to 4.2-fold at 8 hours after injection. The differences were statistically significant at all time-points compared to vehicle treated mice. CGK733 also induced increases in reporter activity over control mice, with 2.4-fold, 3.1-fold, and 1.3-fold changes observed at 1, 4, and 8 hours, respectively. Although both the 1 hour and 4 hour treatment with CGK733 treatment were significantly different from control mice, the 8 hour values returned to near control levels. The observed persistent inhibition of

ATM *in-vivo* compared to the *in vitro* data is likely due to the drug being injected in the peritoneum, which is slowly and continually absorbed into the bloodstream over hours, thus creating prolonged ATM inhibition in tumors.

A group of mice were also treated with radiation to their flank tumors (5 Gy) and changes in bioluminescence compared to sham-treated mice were monitored over time (Fig. 6C). Similar to the *in vitro* data, radiation induced a decrease in reporter activity as early as 1 hour after radiation, with a 0.82 fold-reduction of control values (or a 18% decrease). At 4 and 8 hours, decreases in reporter activity were sustained compared to control mice, with a fold-reduction to 0.28 and 0.33 of control values at 4 and 8 hours, respectively ($p<0.05$). To validate these results, tumor tissue was analyzed after control, KU-55933 (25 mg/kg), or radiation (5 Gy) and by immunoblotting. As demonstrated in Fig 6D, KU-55933 resulted in a decrease in both p-ATM and p-Chk2 at 1 and 8 hours compared to control tumors. In addition, treatment with 5 Gy resulted in activation of Chk2 and phosphorylation of H2A.X (a core histone that is phosphorylated by kinases including ATM in response to DNA damage), which correlated with bioluminescence activity at 1 and 8 hours. It is well-characterized that activation of ATM is a rapid process after ionizing radiation, with p-ATM detected early (within 15 minutes) in cells. The same is true of nuclear p-ATM foci (indicative of DNA damage).

Discussion

In this report, we describe the development and validation of a novel reporter molecule designed to monitor ATM kinase activity in living cells and animals. We observed that ATM inhibition resulted in activation of the reporter in a dose-dependent fashion. In addition, ionizing radiation diminishes reporter activity in a time and dosedependent manner that correlates with ATM kinase activity by Western blotting. The timescale of reporter activity is consistent with the known timescale of ATM activation and foci formation after radiation, with rapid activation of ATM and foci formation within 15 minutes which is sustained over 1–2 hours before ATM substrate Chk2 activity begins to return to normal. Furthermore, we showed that the reporter could be successfully targeted to the nucleus (where the predominant sub-cellular and biologically relevant location of ATM activity resides). As predicted, targeting of the reporter to the nucleus enhanced its sensitivity to both ATM inhibitors and activation of ATM through ionizing radiation. A mutant ATM reporter defective in an SQ/TQ motif of the Chk2 peptide consensus sequence rendered the reporter substantially less responsive. Additionally, we show that the ATMR is specific for ATM kinase activity, through the use of targeted knockdown of ATM expression, as well as through application of a highly specific molecular inhibitor of ATM, KU-55933. Lastly, we demonstrate that the reporter can be successfully applied for *in vivo* studies.

In summary, we have developed ATMR that enables quantitative imaging of ATM kinase activity in real-time and non-invasively. We improved reporter sensitivity by targeting it to the nucleus. The reporter will be invaluable in measurement of the DNA damage response pathway, to perform cell-based high-throughput screening to identify novel ATM inhibitors, to perform siRNA library screening to identify novel ATM- or Chk2-pathway modulating genes. In addition, unlike FRET-based reporters [8], ATMR provides the ability to evaluate pharmacokinetics/pharmacodynamics of known or novel ATM inhibitors, or to rationally design (i.e. through optimal dosing and scheduling) and compare the efficacy of therapeutic regimens employing ATM inhibitors and/or radiation in living subjects.

Supplementary Material

Refer to Web version on PubMed Central for supplementary material.

Acknowledgments

We would like to thank Swaroop Bhojani and Christine Canman for technical support and advice and Steven Kronenberg for generating figures. This work was supported by NIH research grants R01CA129623 (A.R.), P50CA093990 (B.D.R and A.R.), and by RSNA Research Resident/Fellow Grant and a Conquer Cancer Foundation Young Investigator Award (to T.M.W.). T. M. Williams was designated a B. Leonard Holman Pathway Resident by the American Board of Radiology.

References

1. Ahn JY, et al. Threonine 68 phosphorylation by ataxia telangiectasia mutated is required for efficient activation of chk2 in response to ionizing radiation. Cancer research. 2000; 60:5934–5936. [PubMed: 11085506]
2. Bao S, et al. Glioma stem cells promote radioresistance by preferential activation of the DNA damage response. Nature. 2006; 444:756–760. [PubMed: 17051156]
3. Bartkova J, et al. DNA damage response as a candidate anti-cancer barrier in early human tumorigenesis. Nature. 2005; 434:864–870. [PubMed: 15829956]
4. Choudhury A, Cuddihy A, Bristow RG. Radiation and new molecular agents part i: Targeting atm-atr checkpoints, DNA repair, and the proteasome. Semin Radiat Oncol. 2006; 16:51–58. [PubMed: 16378907]
5. Durocher D, Jackson SP. The fha domain. FEBS Lett. 2002; 513:58–66. [PubMed: 11911881]
6. Gately DP, et al. Characterization of atm expression, localization, and associated DNA-dependent protein kinase activity. Molecular Biology of the Cell. 1998; 9:2361–2374. [PubMed: 9725899]
7. Hickson I, et al. Identification and characterization of a novel and specific inhibitor of the ataxia-telangiectasia mutated kinase atm. Cancer Res. 2004; 64:9152–9159. [PubMed: 15604286]
8. Kalderon D, et al. A short amino acid sequence able to specify nuclear location. Cell. 1984; 39:499–509. [PubMed: 6096007]
9. Lavin MF. Ataxia-telangiectasia: From a rare disorder to a paradigm for cell signalling and cancer. Nat Rev Mol Cell Biol. 2008; 9:759–769. [PubMed: 18813293]
10. Luker KE, et al. Kinetics of regulated protein-protein interactions revealed with firefly luciferase complementation imaging in cells and living animals. Proceedings of the National Academy of Sciences of the United States of America. 2004; 101:12288–12293. [PubMed: 15284440]
11. Perona R, et al. Role of chk2 in cancer development. Clin Transl Oncol. 2008; 10:538–542. [PubMed: 18796370]
12. Sarkaria JN, et al. Inhibition of atm and atr kinase activities by the radiosensitizing agent, caffeine. Cancer research. 1999; 59:4375–4382. [PubMed: 10485486]
13. Shiloh Y. Atm and related protein kinases: Safeguarding genome integrity. Nat Rev Cancer. 2003; 3:155–168. [PubMed: 12612651]
14. Won J, et al. Small molecule-based reversible reprogramming of cellular lifespan. Nat Chem Biol. 2006; 2:369–374. [PubMed: 16767085]
15. Won JJ, et al. Small molecule-based reversible reprogramming of cellular lifespan. Nature chemical biology. 2006; 2:369–374.
16. Zhang L, et al. Molecular imaging of akt kinase activity. Nature medicine. 2007; 13:1114–1119.

SUMMARY

We report the development, characterization, and validation of a luciferase-based reporter which enables the non-invasive measurement of ATM-kinase activity. This reporter molecule provides the ability to monitor the DNA damage response, and thus serve as an invaluable tool to provide unique biological insights into radiation-induced signaling events in live cells and animals.

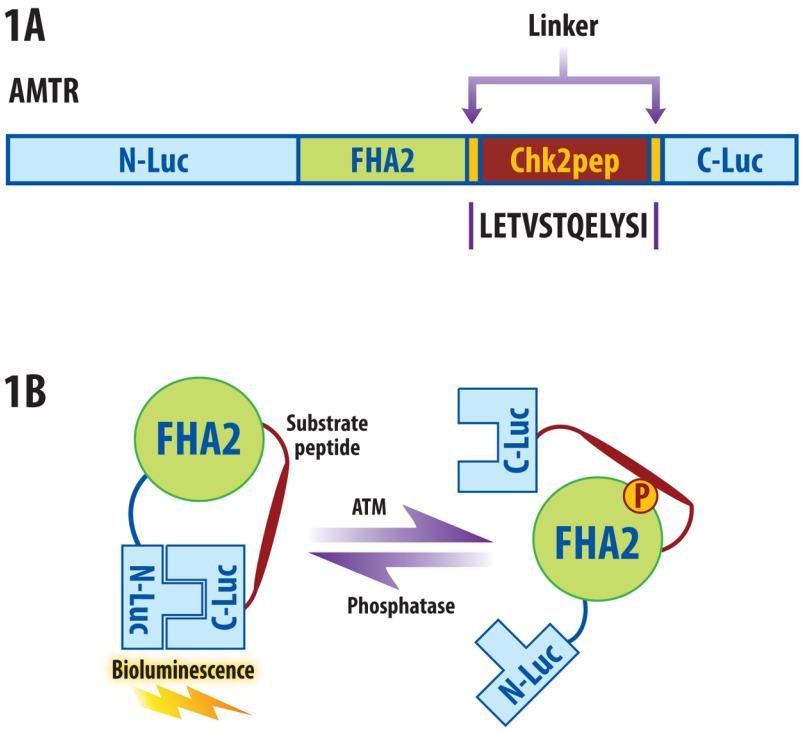

Figure 1.
ATM reporter (ATMR). (a) The domain structure of the ATMR. The N-Luc and C-Luc fragments of firefly luciferase flank an FHA2 phosphopeptide binding domain and 12 amino acid Chk2 substrate peptide. (b) The proposed mechanism of action for the ATM reporter involves ATM-dependent phosphorylation of the Chk2 peptide (thick line), which results in interaction of the FHA2 domain (right). In this form, the reporter has minimal bioluminescence activity. In the absence of ATM kinase activity, the N-Luc and C-Luc domains re-associate, restoring bioluminescence activity (left).

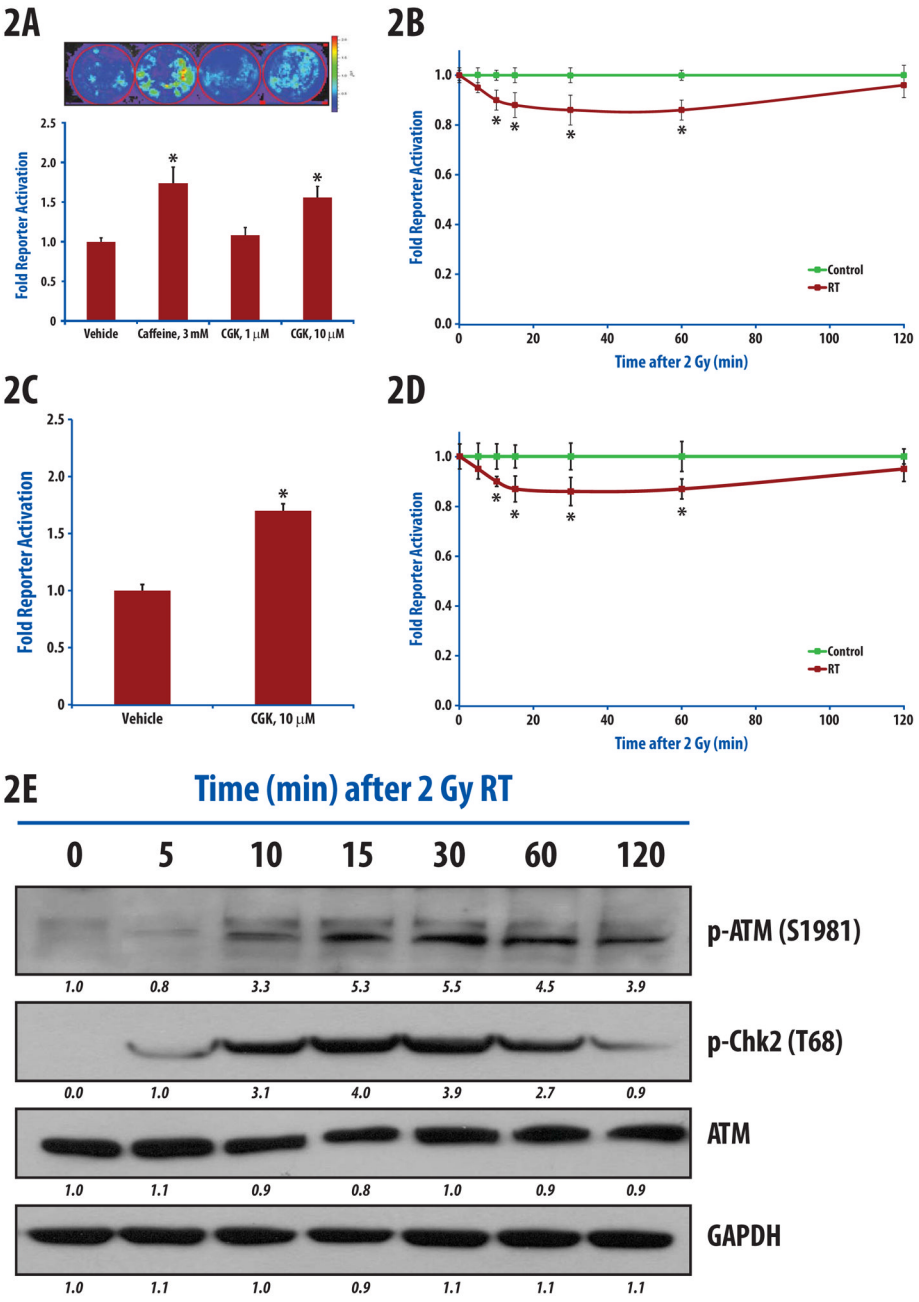

Figure 2.

Treatment dependent changes in ATM kinase. (a) 293-ATMR cells were treated for 1hr with either vehicle, caffeine (3 mM), or CGK-733 (1 μM, 10 μM), bioluminescent activity was measured and normalized to vehicle-treated cells and expressed as fold activation. (b) 293-ATMR cells were irradiated (2 Gy) and bioluminescent activity was monitored at 5, 10, 15, 30, 60, and 120 min post- irradiation. (c) D54-ATMR cells were treated with vehicle or CGK-733 (10 μM). (d) D54-ATMR cells were irradiated (2 Gy) and reporter activity was monitored at 5, 10, 15, 30, 60, and 120 min after radiation. (e) Western blotting of phospho-ATM (Ser1981), phospho-Chk2 (Thr68), and ATM in 293-ATMR cells after irradiation (2 Gy) at various times. Asterisks indicate p-value < 0.05 compared to control cells. Error bars are s.e.m. Quantification of western blot intensities was performed using ImageJ.

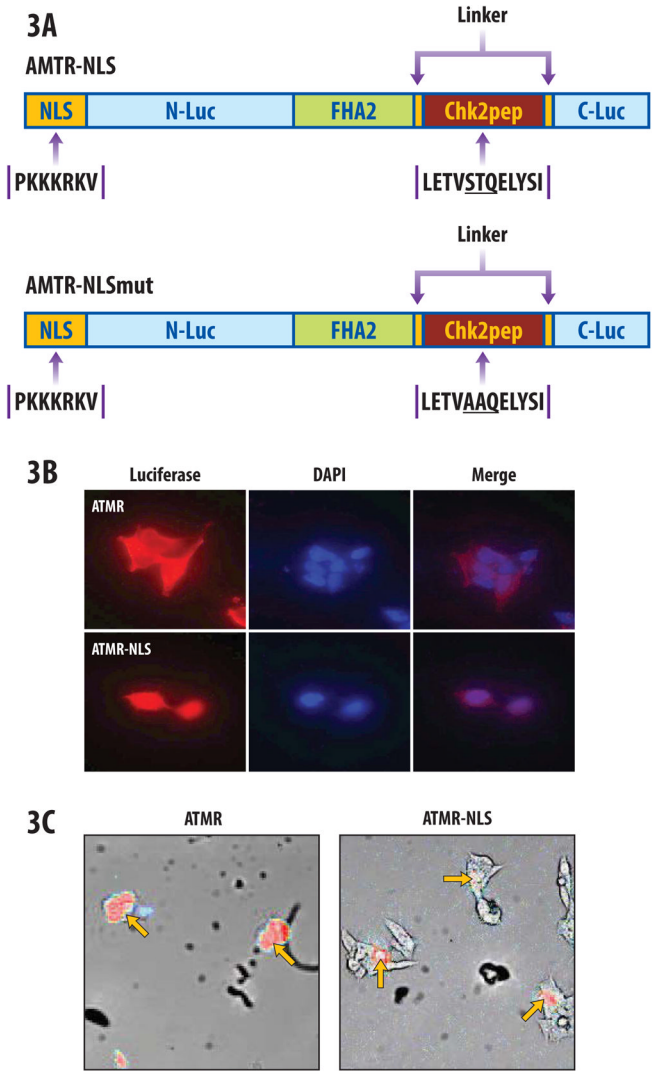

Figure 3.

Nuclear-targeted ATM reporter (ATMR-NLS). (a) Schematic depiction of ATMR-NLS and mutant constructs, bearing a nuclear localization signal (NLS). (b) Immunocytochemistry with anti-luciferase antibody illustrating nuclear targeting of ATMR-NLS reporter molecules in 293-ATMR-NLS cells (bottom panels), compared to the ATMR in 293-ATMR cells (top panels) at 40X. DAPI is shown as a nuclear counterstain. (c) Single-cell bioluminescent imaging demonstrating diffuse (cytoplasmic and nuclear) staining in ATMR (left panel), or nuclear localization in ATMR-NLS cells (red color, red arrow, right panel) at 20X magnification.

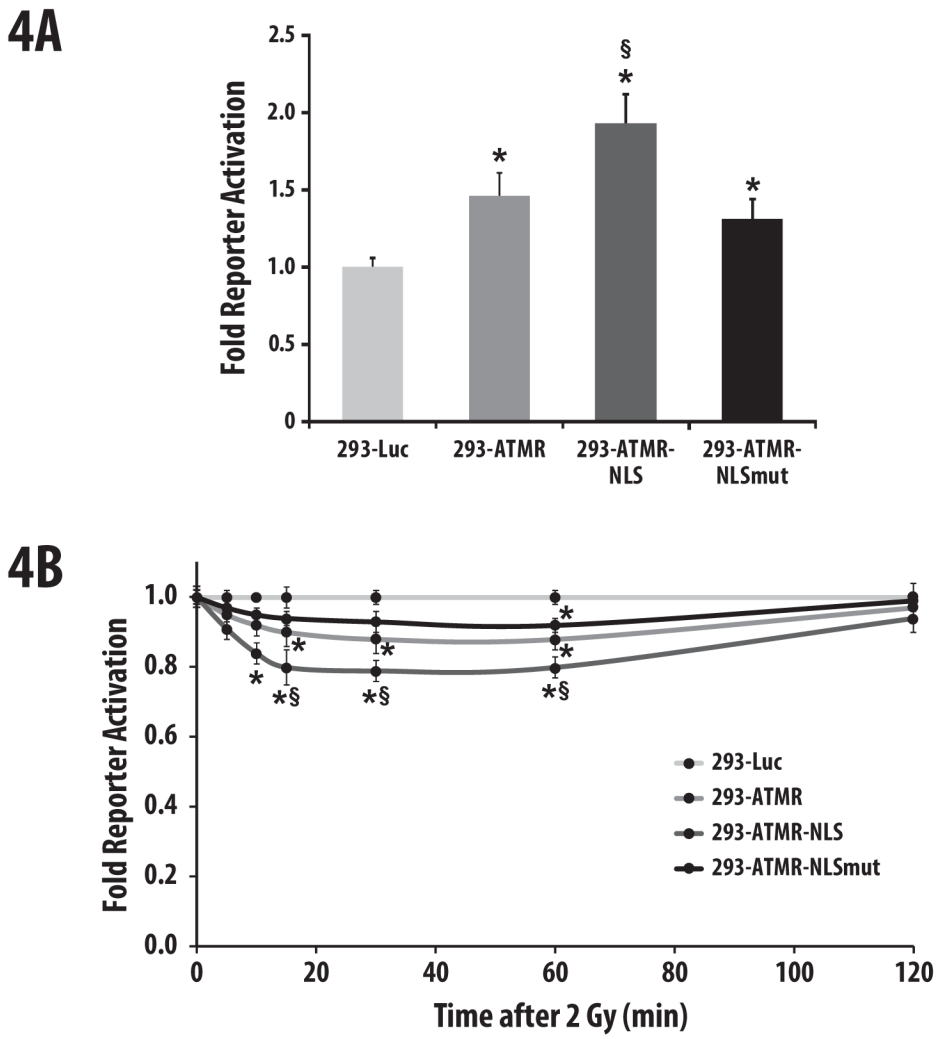

Figure 4.

ATMR-NLS demonstrates enhanced sensitivity compared to the ATMR. (a) Treatment of 293 cells bearing either a control luciferase (Luc), ATMR, ATMR-NLS, or ATMR-NLSmut for one hour with CGK-733 (10 μM), followed by assaying for bioluminescence. (b) 293 cells bearing various reporters were irradiated with 2 Gy and bioluminescent activity was monitored at 5, 10, 15, 30, 60, and 120 min after radiation. Data are normalized to values from 293-Luc cells, asterisks indicate p-value < 0.05 compared to 293-Luc cells, and § indicates p-value < 0.05 compared to 293-ATMR cells. Error bars are s.e.m.

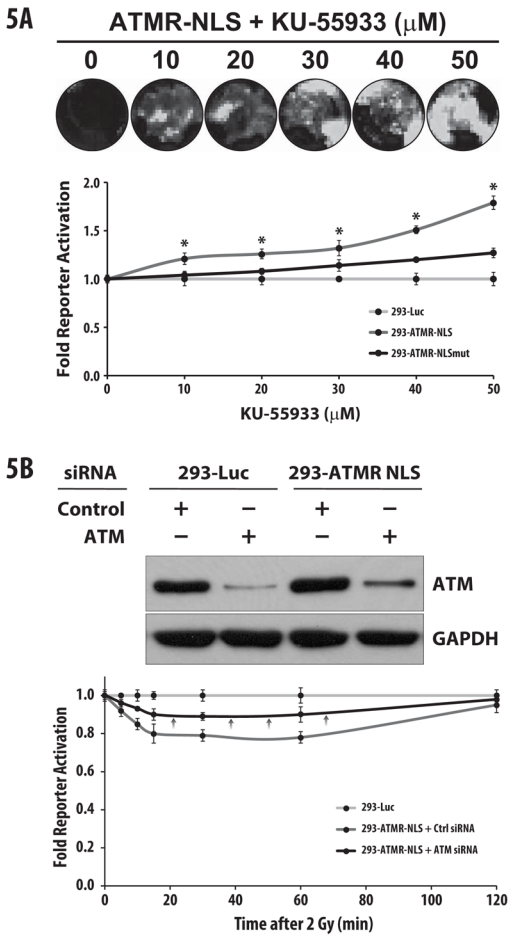

Figure 5.

The ATMR-NLS reporter is specific for ATM activity. (a) 293-Luc, ATMR-NLS, or ATMR-NLSmut cells were treated with increasing concentrations KU-55933 for 1hr. ATMR-NLS cells show a dose-dependent increase in reporter activity compared to other reporters (top panel shows representative image). (b) Treatment of 293-ATMR-NLS cells with ATM siRNA caused target knockdown, as demonstrated by Western blots. 72 hours after siRNA transfection, cells were treated with 2 Gy radiation, and subjected to bioluminescence assays at the indicated time points. Pre-treatment with ATM siRNA resulted in substantial decline in reporter response after treatment with radiation (see black arrows). For both experiments (a) and (b), data are normalized to values from 293-Luc (control) cells, and asterisks indicate p-value < 0.05 compared to control cells. Error bars s.e.m.

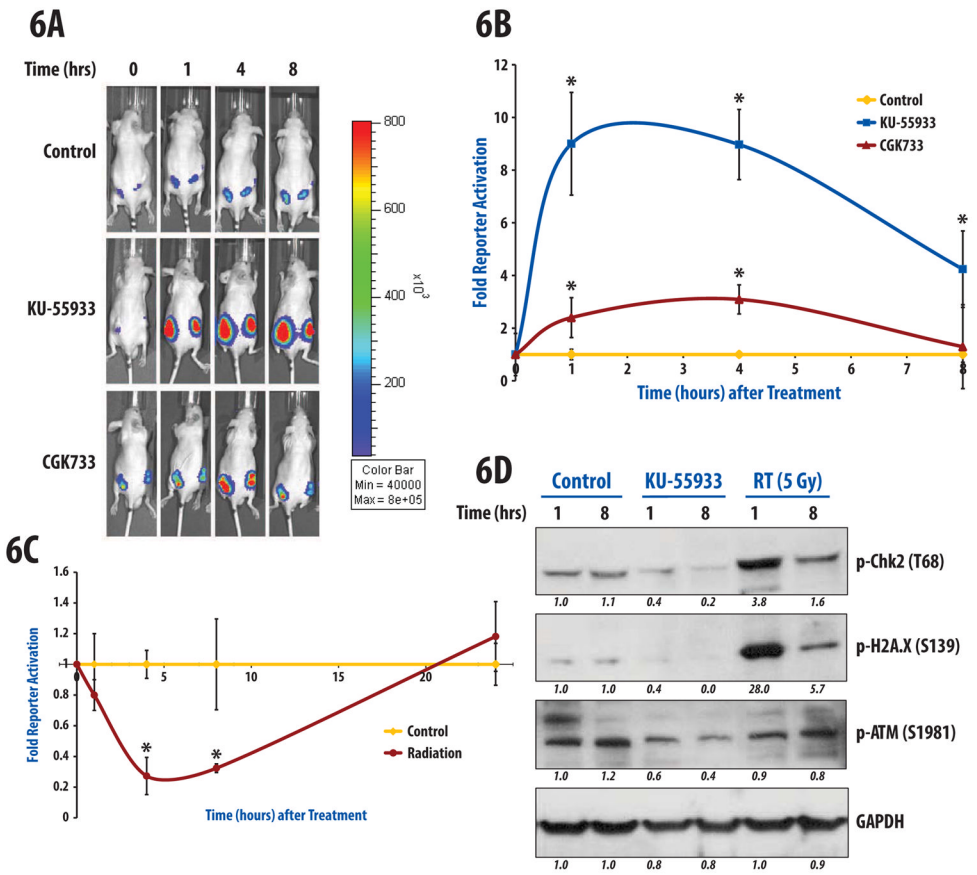

Figure 6.

Molecular imaging of ATM activity *in vivo*. D54-ATMR cells were subcutaneously implanted in the flanks of athymic nude mice and allowed to form tumors. (a, b) Bioluminescence activity was obtained at baseline (0 hr) for all groups (n=5/group), and then treated with vehicle (DMSO), CGK-733 (25 mg/kg), or KU-55933 (25 mg/kg). Reporter activity was measured at 1, 4, and 8 hr after administration of drug. Data are normalized to vehicle-treated mice. The most marked differences were observed after treatment with KU-55933, an ATM specific inhibitor, with peak reporter activation detected at 1 hour post-treatment. (c) Similarly after acquiring baseline bioluminescence activity, animals were either sham (n=5) or irradiated with 5Gy (n=5) and reporter activity was monitored after 1, 4, 8 and 24hr. Significant differences were observed at 4 and 8 hours. Error bars displayed for (b) and (c) are s.e.m. (d) Immunoblotting of lysates derived from D54 flank tumors harvested 1 and 8 hours after DMSO, KU-55933 (25 mg/kg), or radiation (5Gy) was performed with antibodies against phospho-ATM (Ser1981), phospho-Chk2 (Thr68), and phospho-H2A.X (Ser139). Quantification of western blot intensities was performed using ImageJ.